ARTICLE

GDF6, a Novel Locus for a Spectrum of Ocular Developmental Anomalies

Mika Asai-Coakwell,* Curtis R. French,* Karyn M. Berry, Ming Ye, Ron Koss, Martin Somerville, Rosemary Mueller, Veronica van Heyningen, Andrew J. Waskiewicz, and Ordan J. Lehmann

Colobomata represent visually impairing ocular closure defects that are associated with a diverse range of developmental anomalies. Characterization of a chromosome 8q21.2-q22.1 segmental deletion in a patient with chorioretinal coloboma revealed elements of nonallelic homologous recombination and nonhomologous end joining. This genomic architecture extends the range of chromosomal rearrangements associated with human disease and indicates that a broader spectrum of human chromosomal rearrangements may use coupled homologous and nonhomologous mechanisms. We also demonstrate that the segmental deletion encompasses *GDF6,* encoding a member of the bone-morphogenetic protein family, and that inhibition of gdf6a in a model organism accurately recapitulates the proband's phenotype. The spectrum of disorders generated by morpholino inhibition and the more severe defects (microphthalmia and anophthalmia) observed at higher doses illustrate the key role of *GDF6* in ocular development. These results underscore the value of integrated clinical and molecular investigation of patients with chromosomal anomalies.

Normal ocular development entails a series of tightly choreographed events, of which fusing the edges of the optic cup's embryonic fissure represents a key step in forming the future spherical eye. Disruption of this process results in colobomata (MIM 120200)—congenital anomalies affecting tissues in the posterior (retina, choroid, and optic nerve) and anterior (cornea, iris, and lens) ocular segments. Colobomata may, in turn, cause abnormal morphogenesis of other ocular tissues, because of the retina's inductive role in lens formation. Consequently, colobomata are frequently associated with ocular malformations, including cataract, microphthalmia, and anophthalmia; systemic anomalies—such as renal anomalies, mental retardation, and CHARGE (coloboma, heart defects, choanal atresia, retarded growth, and genital and ear anomalies [MIM 214800])[1]—are also observed in a small subset. Causal mutations for coloboma have been identified in only a small number of cases, and the genetic heterogeneity (*OTX2* [MIM 600037],[2] *SHH* [MIM 600725],[3] *MAF* [MIM 177075],[4] *CHX10* [MIM 142993],[5] *CHD7* [MIM 608892],[6,7] and *PAX6* [MIM 607108][8]) reflects the diverse molecular interactions that control eye development. Although autosomal dominant, recessive, and X-linked inheritance[9–11] of colobomata are observed, the absence of clear Mendelian inheritance patterns indicates the presence of a less straightforward molecular basis in some cases.[2,12,13] Increasing the proportion of colobomata with a defined genetic origin would benefit the understanding of complex disease and provide novel insight for ocular development and may identify therapeutic targets for a frequently blinding disorder.

Colobomata are associated with rearrangements affecting at least 10 autosomes,[3–6,8,12,14–17] including several syndromes, such as CHARGE,[7,6] "Cat eye" syndrome (MIM 115470),[17,18] Jacobsen syndrome (MIM 147791),[19] and Wolf-Hirschhorn syndrome (MIM 194190).[16] Study of chromosomal anomalies has proved a fruitful means of identifying dosage- or position effect–sensitive genes, particularly for ocular disorders, since research is facilitated by the fact that the eye is composed of an interface of embryonically distinct tissues and by accessibility to detailed phenotyping.[20–23] Detection of a segmental deletion syntenic with the murine ocular malformation locus *Tcm*[24,25] in a patient with colobomata enabled us to investigate the cause of the ocular developmental phenotype and the mechanism mediating this chromosomal rearrangement. Observation of features of nonallelic homologous recombination (NAHR) and nonhomologous end joining (NHEJ) in this segmental deletion extend the range of chromosome rearrangements associated with human disease. Analyses of genes within and adjacent to the segmental deletion led us to identify *growth differentiation factor 6* (*GDF6* [MIM 601147]) as a candidate gene for the patient's ocular phenotype. Morpholino inhibition of the function of *gdf6* in zebrafish, performed to evaluate this gene's role in retinal development, recapitulated the patient's phenotype.

Material and Methods

Patients

Peripheral-blood samples were obtained from a family in which ocular and systemic developmental anomalies had been identi-

From the Departments of Ophthalmology (M.A.-C.; M.Y.; O.J.L.), Biological Sciences (C.R.F.; K.M.B.; R.K.; A.J.W.), and Medical Genetics (M.A.-C.; M.Y.; M.S.; R.M.; O.J.L.), University of Alberta, Edmonton; and Medical Research Council Human Genetics Unit, Edinburgh (V.v.H.)

Received July 31, 2006; accepted for publication November 28, 2006; electronically published December 29, 2006.

Address for correspondence and reprints: Dr. Ordan J. Lehmann, Departments of Ophthalmology and Medical Genetics, 8–29 Medical Sciences Building, University of Alberta, Edmonton, Alberta, Canada T6G 2H7. E-mail: olehmann@ualberta.ca

* These two authors contributed equally to this work.

Am. J. Hum. Genet. 2007;80:306–315. 0002-9297/2007/8002-0011$15.00

fied in one individual. In view of the breadth of the phenotype, karyotyping of the proband and her parents was undertaken, together with subsequent multiplex-FISH (M-FISH) analysis. This study was approved by the University of Alberta Hospital Health Research Ethics Board, and informed consent was obtained from all participants.

Defining the Segmental Deletion

After initial karyotyping (at the University of Alberta Hospital Cytogenetics Laboratory) revealed a chromosome 8q segmental deletion, M-FISH was undertaken using region-specific and partially overlapping chromosome probes (mBAND X Cyte8 probe set [MetaSystems]).[26] Each contains a unique fluorochrome, which permits quantitative analysis of fluorescence intensity along a chromosome. The deletion's extent was next refined by fluorescent microsatellite-marker genotyping (centromeric: *D8S1697, D8S1702, D8S1838, D8S461, D8S1912,* and *D8S1119*; telomeric: *D8S1699, D8S1127, D8S1772, D8S1129,* and *D8S1778*). Subsequently, comparative genomic hybridization (CGH) was performed with a custom array comprising isothermal, long oligonucleotide probes tiled at a 5-kb density across the repeat-masked genomic interval encompassing the segmental deletion (Nimblegen). The mean probe density was increased to 1 kb in regions predicted by microsatellite-marker genotyping to correspond to the centromeric and telomeric breakpoints. CGH was performed as described elsewhere,[27] with use of the proband's DNA labeled with Cy3, hybridized with a Cy5-labeled reference DNA.

Amplification of the Junctional Fragment

Guided by the CGH results and bioinformatic sequence information, multiple primer pairs were designed to amplify a junctional fragment that spanned the segmental deletion. One of these nine primer permutations (F2-R3) yielded an amplicon in the proband, through use of long-range PCR (Elongase [Invitrogen]), which was purified with Montage (Millipore) and was sequenced using these and internal primers (table 1), with a BigDye (v3.1) terminator kit and 3100 DNA sequencer (Applied Biosystems). Subsequent *in silico* analyses of the sequence adjacent to the breakpoint were performed with Ensembl, University of California–Santa Cruz (UCSC), and National Center for Biotechnology Information (NCBI) Entrez genome browsers. Through use of BLASTn (NCBI BLAST),[28] homologous sequences adjacent to the breakpoint were identified, and the boundaries of the repeat elements were determined using PipMaker[29] and Ensembl, UCSC, NCBI Entrez, and NCBI BLAST.

Bioinformatic and Expression Analyses

Database analyses of genes lying in the deleted region or adjacent to the breakpoints were performed to identify candidate(s) for the ocular phenotype (Ensembl, UCSC, and UniGene). FISH was also undertaken with the BAC clone RP11-516P9, to validate database predictions. The expression of one gene (*GDF6*) was investigated by RT-PCR of murine (adult and embryonic) and zebrafish (18 and 42 h postfertilization [hpf]) tissue (through use of primers shown in table 1 and Superscript III RT-PCR [Invitrogen]). Ethidium bromide–stained amplicons were visualized on 1% agarose gels. Whole-mount in situ hybridization was undertaken using digoxigenin-labeled antisense RNA probes specific to retinal developmental genes that are primarily markers of regional identity. cDNA from *hmx3b* (*nkx5.1*/*soho1*), *aldh1a2* (*raldh2*), and *foxg1* were generated, and in situ hybridization was performed as described elsewhere[30] on wild-type and *gdf6a*-morphant zebrafish.

Analysis of gdf6a *Function in Zebrafish*

Zebrafish possess two orthologues, *gdf6a* (*radar*) and *gdf6b* (*dynamo*),[31] with *gdf6a* expressed in developing retina, dorsal fin, dorsal neural tube, and posterior endoderm.[32,33] Zebrafish embryos have two sources of gdf6a: unspliced zygotic and prespliced maternal gdf6a mRNA. Morpholino inhibition of zebrafish zygotic *gdf6a* function results in cranial and dorsal neural-tube apoptosis, whereas inhibition of both maternal and zygotic *gdf6a* (with a translation-blocking morpholino) generates an earlier dorsalized phenotype, thereby preventing analysis of eye development.[34] Accordingly, two splice-blocking morpholino antisense oligonucleotides (MOs) were designed to independently target gdf6a splicing, which enables comparison of the phenotype generated by each. The first (*gdf6a*^{MO1}) targets the 5′ splice site, whereas the second (*gdf6a*^{MO2}) targets the intron 1–exon 2 boundary. Additional morpholinos were designed to target the translation start site of *gdf6b* (*gdf6b*^{MO}) and to provide a capability to reduce apoptotic cell death to the translation start site of *p53* (*p53*^{MO}). Oligonucleotides *gdf6a*^{MO1} (GCAATACAAACCTTTTCCCTTGTCC),[34] *gdf6a*^{MO2} (GAGATCGTCTGCAAGATAAAGAGAA), and *p53*^{MO} (GCGCCATTGCTTTGCAAGAATTG)[35] were provided by Gene Tools; *gdf6b*^{MO} (TCAAAAGTATCCCGCAGGCACACAT) was provided by Open Biosystems. The efficiency of the two *gdf6a* morpholinos was evaluated by RT-PCR of mRNA derived from 18-hpf uninjected and morphant embryos, by use of *gdf6a* primers spanning the intron (table 1). Zebrafish (AB strain) were obtained from the zebrafish stock center ZIRC and were maintained under stan-

Table 1. Primers Used to Amplify the Chromosome 8q22 Junctional Fragment and for RT-PCR of Murine and Zebrafish *gdf6*

Analysis	Primer (5′→3′) Forward	Primer (5′→3′) Reverse	Annealing Temperature (°C)
Fragment:			
F2-R3	CCATGACGTGTGAAACCAAC	TCATTGGTCTGGGTAGAGC	60
Chromosome 8-4	AGGCACAACAGGAAATGAAGTT	GTTGACACTCCTTCCCTCCA	60
Chromosome 8-5	GAAGCACTTACATCAGCACCTG	GACCCCATCTCTTATTCTTGCTT	60
Chromosome 8-6	TAGGCTGCCTGAGTGTCCTT	GGTTCGTGGTCTCACTGGTT	60
RT-PCR:			
Murine	GCGCGTGGTGCCTCACGAGTAC	GGGGCGCGATAATCCAGTCGTC	60
Zebrafish	CGCGGTCCAAGAAGAGAGAGAACTT	GCGCGTCTTTACGCATCGTTCAAGT	60
gdf6a	GTGAGACACGGCTCCACTTTACTC	GAAGGTTGTAGACGCCTGATGGGG	55

dard conditions. Morpholino (2–4 nl) was injected into one-cell–stage zebrafish embryos, at a concentration of 2.5 mg/ml, as described elsewhere.[36] All injections of *gdf6a* morpholino included 3 ng of $p53^{MO}$ to reduce apoptotic cell death, a known side effect of morpholino injection. Morphological observations were made with an Olympus SZX12 stereomicroscope and were recorded using a Qimaging micropublisher digital (charged-couple device) camera. For histological analysis, larvae were fixed in a 2.5% glutaraldehyde, 1% paraformaldehyde mix, followed by 4% osmium tetroxide, embedded in Epon, and a thin (1 μm) section cut with an ultramicrotome. Richardson's and phalloidin stains were used to visualize structural details within the retina and surrounding tissues.

Results

Phenotype

The proband exhibited multiple developmental defects, including neurodevelopmental impairment (performance IQ 74), bilateral soft-tissue syndactyly of the 2nd and 3rd toes, an atrial septal defect, and ocular malformations (fig. 1). The latter comprised bilateral retinochoroidal colobomata with optic-nerve involvement (fig. 1*A* and 1*B*), plus a unilateral iris coloboma (fig. 1*C*), which reduced vision to counting fingers and 20/50 in the right and left eyes, respectively. Although the proband's father was asymptomatic, ocular examination revealed features of much milder developmental defects that included a minor degree of optic-nerve dysplasia, anomalous retinal vascular branching, and small retinochoroidal colobomata (fig. 1*G* and 1*H*). The changes were associated with corrected acuities of $20/20^{-2}$ and 20/30 (normal ~20/20).

Fine Mapping and Sequencing of Breakpoint

Karyotyping identified a chromosome 8q segmental deletion—46,XX, del (8)(q21.2q22.1)—in the proband but in neither parent (data not shown). These findings were confirmed by M-FISH, with the segmental deletion present in all 13 examined metaphase preparations (fig. 1*J*–1*L*). The informativeness of microsatellite-marker genotyping was constrained by the small pedigree size and polymorphism-information-content values of available markers. Nonetheless, it confirmed that the deletion was present in the paternally derived chromosome 8, and the semiquantitative dosage information it provided localized the centromeric and telomeric breakpoints to ~3-Mb regions. CGH accurately defined the extent of the segmental deletion (10.37 Mb) and refined the breakpoint positions to ~10-kb intervals (data not shown). Long-range PCR amplified a 4.5-kb junctional fragment in the proband but in neither parent (fig. 2*C*). Sequence analysis of the junctional fragment revealed the insertion of four nucleotides (AGCT) at the junction of the centromeric and telomeric breakpoints (fig. 2*A* and 2*B*). The telomeric breakpoint lies in a long terminal repeat (LTR) of family MaLR, within a 3.6-kb region of repetitive sequence (fig. 2*A*). The centromeric breakpoint is within an *Alu* element located within a 5.7-kb stretch of contiguous repeats (short interspersed nuclear elements [SINEs], long interspersed nuclear elements [LINEs], LTRs, and simple repeats).

Candidate-Gene and Mutation Analysis

The proband's retinal phenotype and the known molecular conservation of ocular development were used to identify candidate genes *in silico*. Of 31 genes within and 10 adjacent to the segmental deletion, 14 were expressed in both fetal eye and retinal tissue, and, of these, 11 (*CA2, CA3, WWP1, NBN, FAM82B, TMEM64, TMEM55A, UQCRB, PTDSS1, SDC2,* and *GDF6*) had orthologues present in *Fugu* or *Danio*. Because of its involvement in bone morphogenetic protein (BMP) signaling, its developmental role, and the location of *Gdf6* within the *Tcm* locus,[24] *GDF6* was selected for more-detailed study. Subsequent refinement of the *Tcm* locus from a 26-Mb[24] to a 1.3-Mb[25] interval permitted comparison of the five genes or transcripts (unknown, *helicase-related, Cralbp-related, Asph,* and *Gdf6*) within the *Tcm* locus with those encompassed by the segmental deletion. Because of a synteny break between human chromosome 8 and murine chromosome 4, *Gdf6*/*GDF6* is the only gene common to the *Tcm* and chromosome 8q segmental deletion intervals (fig. 2*D*).

Studies of gdf6a *in Zebrafish*

Previous studies have examined the role of *gdf6a* in early dorsal-ventral axis formation, but its function during retinal development remains to be elucidated. The expression of zebrafish *gdf6a* was examined with in situ hybridization and was shown to be specific for the dorsotemporal region of the developing retina at 18 and 24 hpf (fig. 3*A* and 3*B*). The expression pattern of Gdf6 is evolutionarily conserved, as determined by our RT-PCR results of murine retina during early development and the published expression in the dorsal retina of *Xenopus*[37] (data not shown). Splice-blocking *gdf6a* morpholinos were injected into one-cell–stage zebrafish embryos; RT-PCR confirmed that >70% of *gdf6a* mRNA was aberrantly spliced in both $gdf6a^{MO1}$- and $gdf6a^{MO2}$-injected morphants (fig. 3*C*). Morpholino inhibition of *gdf6a* function revealed the axial vasculature, dorsal fin, hypochord, and dorsal neural-tube anomalies (reported elsewhere[32,33]). In situ hybridization with probes to *aldh1a2, hmx3b,* and *foxg1* demonstrated that *gdf6a* morpholinos profoundly altered retinal patterning (fig. 3*D*–3*L*). Expression of *aldh1a2,* a marker of dorsotemporal retina, was completely eliminated in 90% and 97% of $gdf6a^{MO1}$- and $gdf6a^{MO2}$-injected embryos, respectively (n = 113) (fig. 3*D*–3*F*). Expression of *hmx3b,* an early marker of dorsal retina, was strongly reduced in 81% and 85% of $gdf6a^{MO1}$- and $gdf6a^{MO2}$-injected embryos, respectively (n = 110) (fig. 3*G*–3*I*). In contrast, expression of *foxg1,* a marker of ventral-nasal retina, was expanded in 77% and 88% of $gdf6a^{MO1}$- and $gdf6a^{MO2}$-injected embryos, respectively (n = 118) (fig. 3*J*–3*L*). Lenticular expression of *hmx3b* was unaltered in morphant embryos (fig. 3*G*–3*I*). Overall, these results demonstrate that *gdf6a* functions

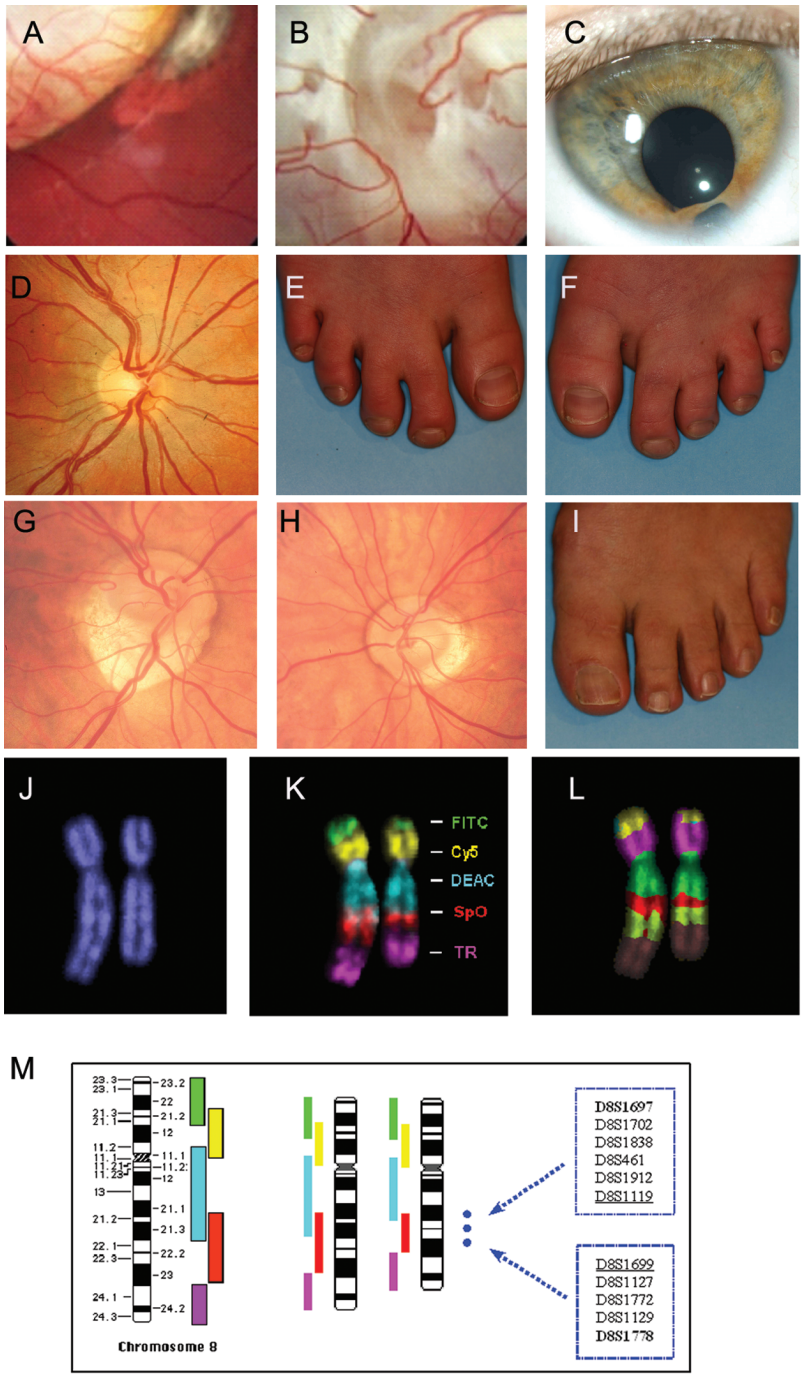

Figure 1. *A–F,* Phenotypes of proband with chromosome 8q segmental deletion who has colobomatous developmental anomalies affecting the anterior and posterior ocular segments (*A*). Note the junction between the normal and abnormal retina. *B,* Retinochoroidal colobomata, with extensive optic nerve involvement. *C,* Iris coloboma (right eye). *D,* Normal optic nerve and retina (for comparison). *E* and *F,* Syndactyly affecting the 2nd and 3rd toes. *G–I,* Phenotypes of the proband's father, demonstrating milder ocular colobomata and syndactyly. *G,* Dysplastic optic nerve with anomalous vascular pattern and small inferior retinochoroidal coloboma. *H,* Similar but milder changes (left eye). *I,* Soft-tissue syndactyly. M-FISH and summary of microsatellite marker genotyping results confirmed chromosome 8q segmental deletion and approximate breakpoint positions. *J,* 4′,6-Diamidino-2-phenylindole staining demonstrating length difference between the undeleted and the segmentally deleted chromosome. *K,* Merged fluorescence signals from five M-FISH probes illustrating the segmental deletion. *L,* "False color" counterstaining, to illustrate with greater clarity the effect of the segmental deletion on length of chromosome 8q. *M,* Montage illustrating normal hybridization pattern for each probe, decreased hybridization for diethylamino-coumarin (DEAC) and SpO, the approximate extent of the segmental deletion (*dotted blue line*), and the microsatellite markers used to refine the breakpoint position. Undeleted markers are shown in bold, deleted markers are underlined, and uninformative markers are shown in plain type.

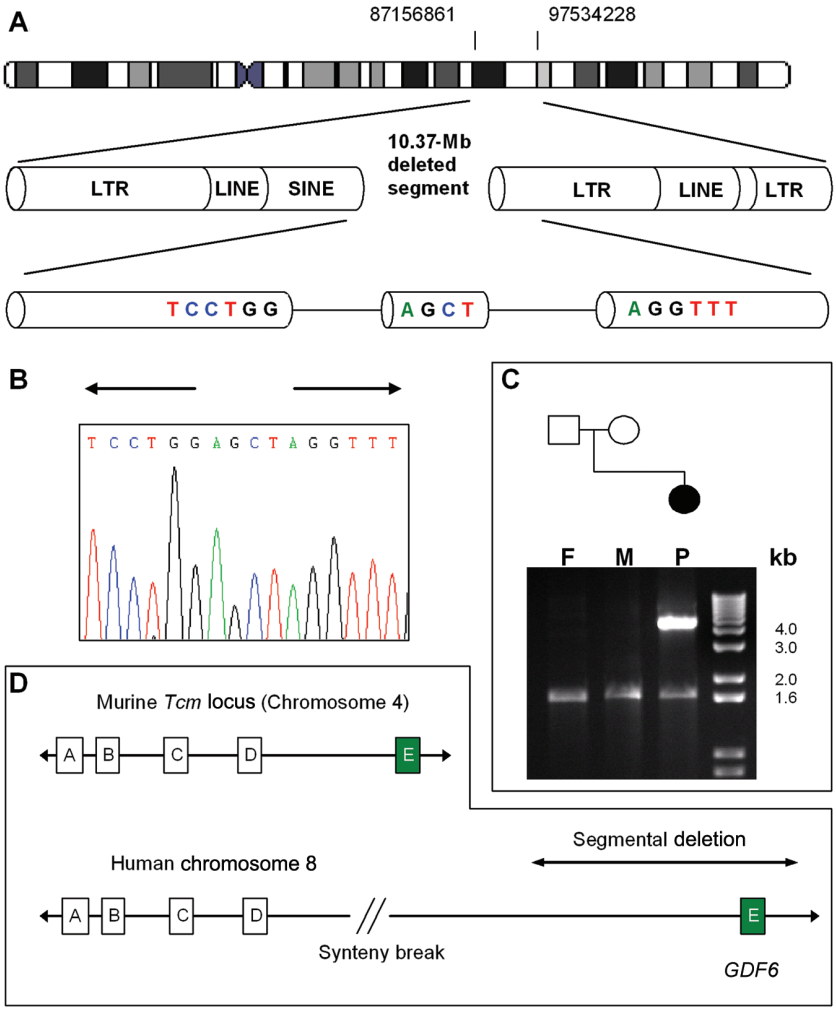

Figure 2. *A,* Schematic representation of the proband's segmental deletion, with coordinates of the centromeric and telomeric breakpoints shown above the representation. *GDF6* is located at positions 97223736–97244196. *B,* Sequence of junctional fragment comprising TCCTGG from the centromeric end, fused to a 4-bp insertion (AGCT), and AGGTTT from the telomeric breakpoint >10 million bp away. The repetitive sequences adjacent to the breakpoints comprise 5.7 kb of repeats centromerically and 3.6 kb of repeats telomerically. (Some repeats extend beyond the depicted region.) *C,* Amplification of a 4.5-kb deletion-junction fragment in the proband that is not present in the unaffected parents (1.7-kb control fragment amplified in all subjects). F = father; M = mother; P = proband. *D,* Murine *Tcm* locus on chromosome 4, a 1.17-Mb region encompassing five genes (A = unknown; B = *helicase-related*; C = *Cralbp-related*; D = *Asph*; E = *Gdf6*) and their orthologues on human chromosome 8. Because of a synteny break, four genes are ~35 Mb centromeric to the segmental deletion, with only *GDF6* common to both.

to specify dorsotemporal retinal identity and to repress ventronasal identity.

In addition, as is evident (fig. 4), *gdf6a* morphants exhibit a range of ocular anomalies that recapitulate the patient phenotype (fig. 1). These features, apparent as early as 18 hpf, include ventral colobomata (35%; $n = 214$, at 48 hpf), persistent dorsal-retinal groove (17%; $n = 214$, at 48 hpf), and decreased ocular and lenticular size (30%; $n = 214$, at 48 hpf) (figs. 4*A,* 4*B,* and 5). In contrast to the declining proportion of morphants observed with colobomatous defects at later stages (ventral coloboma [10% at 72 hpf], dorsal-retinal groove [2% at 72 hpf] [fig. 4*A*–4*D*]), the frequency of lens extrusion and microphthalmia (9% and 60%, respectively, at 120 hpf) increased over time (figs. 4*E*–4*H* and 5). Injection of higher doses of *gdf6a* morpholino cause ocular regression to vestigial structures that resemble human anophthalmia (fig. 4*H*). To investigate retinal development at the cellular level, we examined *gdf6a* morpholino–treated zebrafish embryos histologically. This revealed a consistent reduction in ocular, lenticular, and retinal size, together with prominent defects in both retina and lens (fig. 4*I*–4*L*). Although all cell types are visible, the retina is disorganized, indicating a critical role for *gdf6a* in regulating neural retina cell behavior. Further-

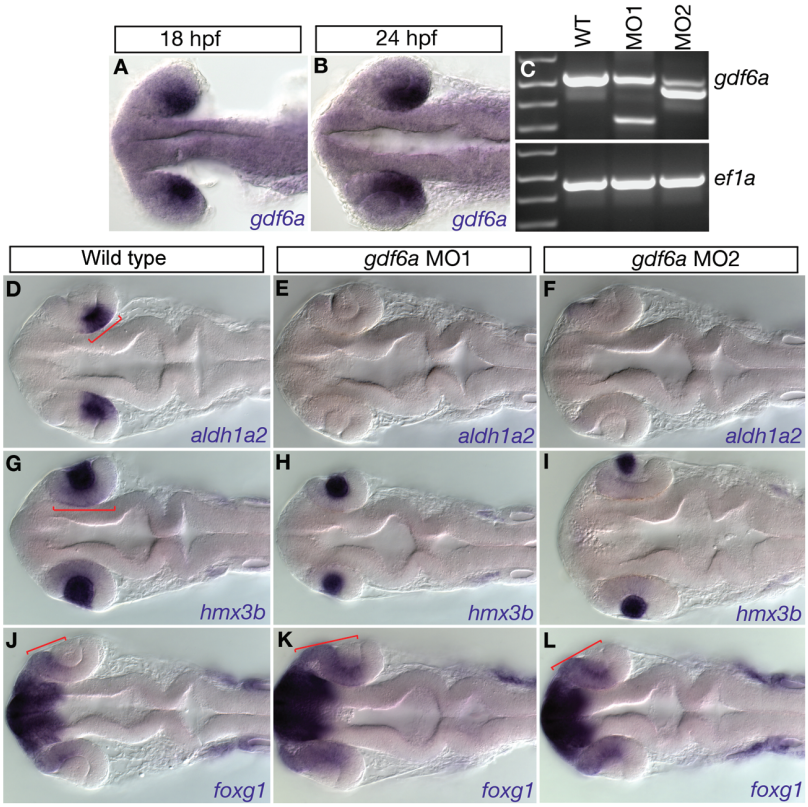

Figure 3. *A* and *B,* In situ analysis of *gdf6a* expression in developing wild-type zebrafish embryos at 18 and 24 hpf. *C,* RT-PCR used to measure spliced *gdf6a* transcripts from uninjected (WT), *gdf6a*^{MO1}-injected (MO1), and *gdf6a*^{MO2}-injected (MO2) embryos, illustrating reduced levels of spliced RNA product in morphant embryos. No change is noted in expression of *ef1a* in either MO1- or MO2-injected embryos. Retinal and lens differentiation was evaluated by examining expression of marker genes in the developing retina at 24 hpf. Expression of *aldh1a2* (*D–F*) in the dorsal-temporal retina is eliminated in embryos injected with either *gdf6a* morpholino. Similarly, expression of *hmx3b* (*G–I*) in the dorsal retina is strongly reduced in *gdf6a* morpholino–injected embryos. Expression of *hmx3b* in the developing lens is largely unaffected in *gdf6a* morphants (*G–I*). Analysis of the nasal marker *foxg1* (*J–L*) was expanded posteriorly to more temporal retinal regions in *gdf6a* morphants. Red brackets highlight the extent of retinal gene expression. Embryos are mounted in dorsal view, with the anterior to the left.

more, we find that the optic nerve is hypoplastic and occasionally absent in morphant embryos (10% of embryos are affected) (fig. 4*J* and 4*L*). In stark contrast to our results with *gdf6a/radar,* inhibition of *gdf6b/dynamo* function revealed no ocular phenotype, which clearly demonstrates the specific role of *gdf6a* in ocular morphology.

Discussion

Although colobomata represent a relatively common developmental anomaly (2.6 in 10,000 births)[38] that account for up to 11% of pediatric blindness,[1] knowledge of the genetic basis remains limited. The identification of additional colobomata-causing genes is thus of value; it improves the understanding of function in both normal development and disease and provides the realistic prospect of elucidating non-Mendelian pathways that contribute to ocular-disease phenotypes. The present study characterizes a novel chromosomal anomaly associated with ocular colobomata, provides strong evidence of the key role of *GDF6* in ocular development, and illustrates the interrelated nature of several ocular-disease phenotypes.

GDF6 is a member of the BMP subfamily of transforming growth factor-beta (TGFβ) signaling ligands, which are involved in the creation of dorsal-ventral axes, specification of neural crest, bone formation, and organogenesis.[39,40] Evidence of involvement of BMP proteins in retinal development is provided by the laminar organization and retinal axon pathfinding defects caused by overexpression of the BMP inhibitor gremlin.[41] However, despite studies of model organisms, the role of BMP signaling in retinal development remains insufficiently characterized, and, in particular, the contribution that BMP mutations make to human ocular disease has not been determined.

Ascribing phenotypic causation to a single candidate gene in a large deleted interval presents challenges. Accordingly, a variety of techniques—including CGH deletion mapping, expression analysis, and study of a zebrafish

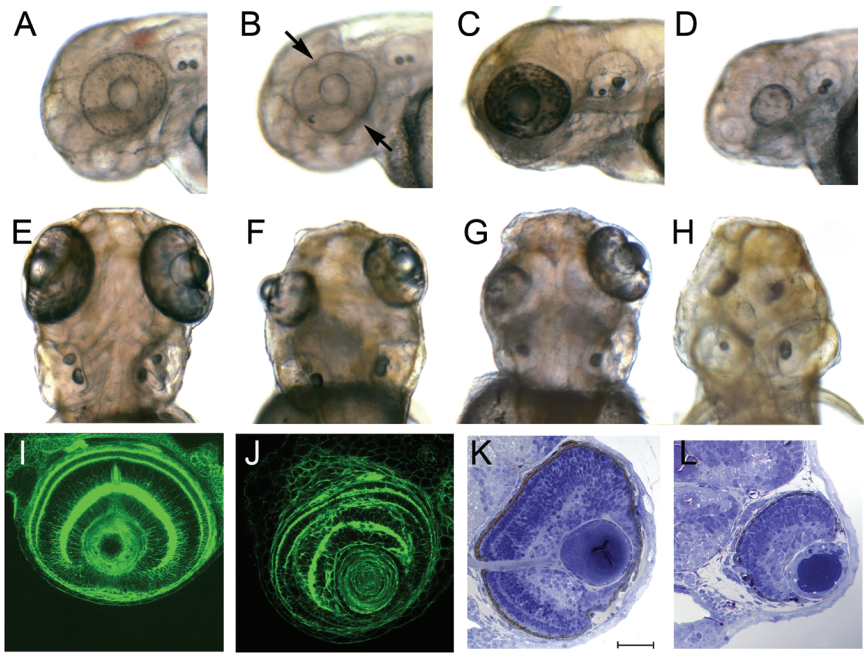

Figure 4. Larval zebrafish retinal defects, caused by injection of splice-blocking *gdf6a* morpholinos. Wild-type images at 48 hpf (*A*) and 72 hpf (*C*), compared with morphant counterparts (*B* and *D*). Decrease in lenticular and ocular size is evident at later stages (*C* and *D*). Ventral colobomata and dorsal groove are highlighted in panel B (*arrows*). *E–H,* Images of 5-dpf zebrafish larvae, illustrating phenotypic variability observed with higher doses (10 ng) of *gdf6a* morpholino (injected at the one-cell stage). *E,* Uninjected control. *F,* Milder phenotype, with unilateral coloboma and lenticular extrusion. *G,* Unilateral coloboma and microphthalmia. *H,* Severe retinal degeneration, resembling human anophthalmia. Transverse histological sections from wild-type (*I* and *K*) and *gdf6a* morphant (*J* and *L*) 3-d-old embryos, with use of phalloidin-Alexa488 and Richardson's stains. Phalloidin-stained images are composites of 12 equally spaced 1-μm sections throughout the eye (*I* and *J*). Note reduction in ocular and lenticular size, loss of normal retinal lamination, and vacuolation of the lens that protrudes anteriorly (*L*). Scale bar = 100 μm.

model of reduced *gdf6a* function—were undertaken, which indicate *GDF6*'s responsibility for the ocular malformations. *Gdf6*/*gdf6*'s expression is temporally and spatially appropriate for a developmental retinal phenotype, and support for its involvement in the observed eye phenotypes is provided by its role in ventral patterning[23]—a process that, when disrupted by *SHH* mutations, also results in colobomata.[3] This accords with decreased *GDF6* copy number (figs. 1 and 2), the eye's exquisite sensitivity to altered gene dosage,[23,42–46] the precise dosage requirement of TGFβ-signaling ligands, and the results of *gdf6a*-morpholino inhibition.

To validate these findings, *gdf6* gene function was inhibited in a zebrafish model. The recapitulation of the proband's phenotype—which generated posterior (dorsal or retinochoroidal) and anterior segment (ventral or iris) colobomata as well as microphthalmia—verifies the key role of *gdf6* and *GDF6* in ocular development. The specificity of these effects is demonstrated by the unaffected lens expression of *hmx3b,* decreased retinal expression of *aldh1a2* and *hmx3b,* and expanded retinal expression of *foxg1* (fig. 3), plus the phenotypic spectrum induced by progressively higher morpholino doses (microphthalmia and posterior-segment colobomata, anterior-segment colobomata, and, finally, anophthalmia) (fig. 4). Furthermore, observation of retina-specific defects at a stage (18 hpf) before retinal vascularization precludes the ocular phenotypes being attributable to nonspecific effects, such as morpholino-induced retinal hypovascularization. Finally, existence of the irradiation-induced *Tcm* mutant, mapping to a small interval containing *Gdf6,* complements the human and zebrafish phenotypes. In view of the fact that only *Gdf6*/*GDF6* is present in both the *Tcm* and segmentally deleted intervals and that *Gdf6*-coding mutations were not observed in *Tcm* mice,[25] the possibility that *Tcm* is allelic and attributable to a segmental anomaly affecting a *Gdf6* regulatory element should be critically evaluated. *Tcm* mice have multiple ocular phenotypes but none of the proband's syndromic features. In contrast, of the two murine $Gdf6^{+/-}$ strains generated, one has only skeletal features described,[47] whereas the other exhibits both skeletal and ocular anomalies (Mouse Genome Informatics [accession number MGI:3604391]), which provides confirmation of the role of *gdf6, Gdf6,* and *GDF6* in eye development.

The effects of zebrafish *gdf6a* inhibition illustrate the interrelated nature of certain ocular phenotypes. In patients, failure of embryonic fissure closure is associated

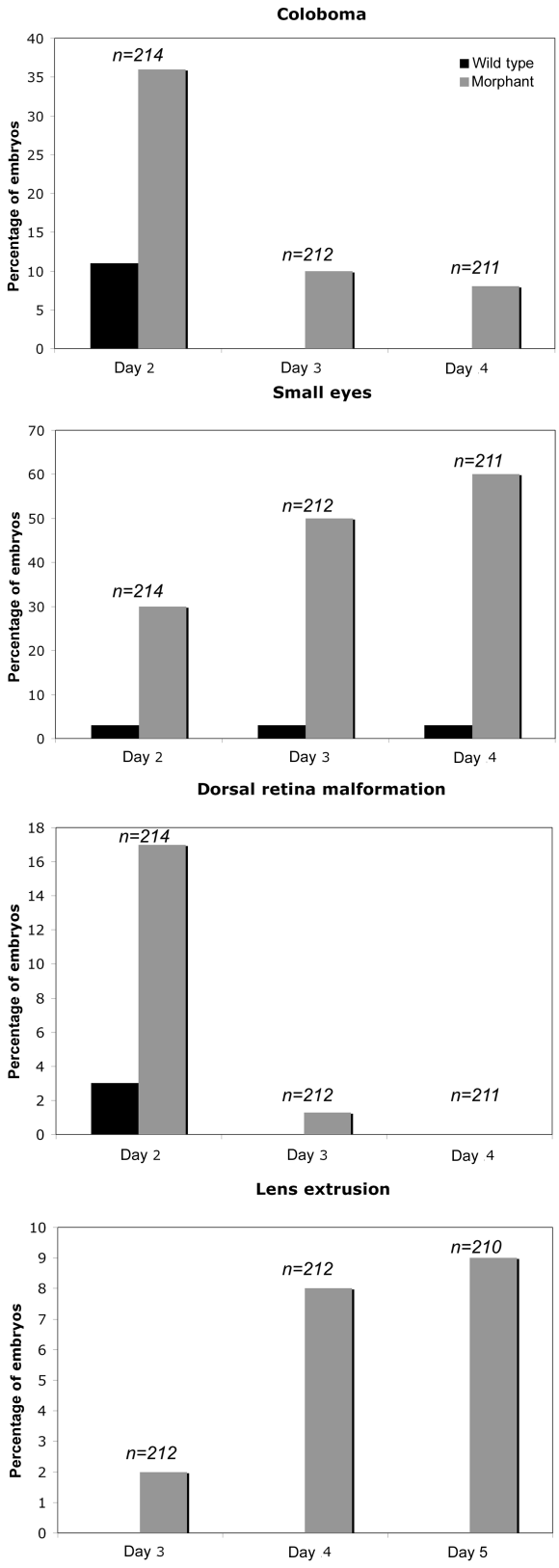

Figure 5. Quantitative ocular phenotypic data from wild-type and *gdf6a* morphant (5 ng *gdf6a*^{MO1} plus 3 ng *p53*^{MO}) embryos at 2–5 dpf.

with variation in ocular size, including microphthalmia, axial length <20 mm (normal 23.5 mm), and anophthalmia (absent eyes or rudimentary ocular remnants). Complementing these clinical observations, in our zebrafish model, more-severe phenotypes were induced with progressively lower *gdf6* levels. In addition to the ocular anomalies, the syndactyly accords with the identical phenotype generated by mutation in the BMP-antagonist *NOGGIN*[48] and *Gdf6*'s role in skeletal development, where null *gdf6* mutations cause carpal and tarsal bone fusion.[47] The same but milder phenotypes present in the proband's father could be compatible with gonosomal mosaicism or chromosomal inversion, and future cytogenetic analyses may differentiate between these possibilities.

Segmental deletions (and duplications) are usually generated by low-copy repeats (LCRs) that provide a substrate for NAHR. Less frequently, NHEJ is responsible, and such rearrangements are characterized by insertion of additional bases at the junction and at breakpoints lying within *Alu* elements or LINEs. The segmental deletion identified in this study exhibits features of both mechanisms. The presence of LTRs on both sides of the deletion indicates intrachromosomal NAHR, whereas the breakpoint's centromeric end's location in an *Alu,* together with insertion of 4 bp, suggests NHEJ. The combination of NAHR and NHEJ has recently been reported in X-chromosomal segmental duplications.[49,50] Observation of NAHR and NHEJ with a segmental deletion extends the range of chromosome rearrangements associated with human disease and indicates that a broader spectrum of human chromosomal rearrangements may use coupled homologous and nonhomologous mechanisms.

In summary, it is evident that *GDF6* has an essential role in retinal development and that altered gene dosage results in a diverse spectrum of ocular malformations. The human and zebrafish phenotypes confirm interspecies conservation of the requirement for precise *GDF6*/*gdf6* dosage in normal development. The studies we have undertaken so far have identified genetic variants that cause substantial functional defects. These ocular phenotypes range from optic-nerve hypoplasia to coloboma/microphthalmia and anophthalmia, which raises the possibility that milder sequence changes contributing to other phenotypes remain to be determined. Availability of zebrafish and murine models, especially *Gdf6*$^{+/-}$ mice in which detailed analysis of the retina has yet to be reported,[47] will facilitate testing of this hypothesis. Equally exciting is the potential for determining the phenotypes associated with reciprocal chromosomal anomalies, exogenous gdf6's ability to rescue induced phenotypes, and the role of other members of the same clade in ocular development and disease. Such investigations, which are just beginning, stem from clinical observation[51,52] of a broader phenotype in a patient with chorioretinal colobomata and may improve understanding of and the outcome for a frequently blinding disorder.

Note Added in Proof.—While this manuscript was under

review, Hanel and Hensey[53] demonstrated inhibition of *Xenopus gdf6* results in ocular developmental phenotypes, providing further confirmation of this gene's important role in vertebrate eye development.

Acknowledgments

We thank the patients for their help with this study; Federic Rosa, Samual Sidi, Mora Robu, and Stephen Ekker, for sharing unpublished information; Dr. Stephen Bamforth, for helpful discussions; and Dr. Garry Drummond, for referring the proband. This work was supported by the Canadian Institutes of Health Research (to A.J.W. and O.J.L.), Alberta Heritage Foundation for Medical Research (to O.J.L.), Canadian Foundation for Innovation (to O.J.L.), and National Scientific Engineering Council and Alberta Ingenuity Fund (to A.J.W.). A.J.W. and O.J.L. are recipients of Canada Research Chairs.

Web Resources

The accession number and URLs for data presented herein are as follows:

Ensembl Genome Browser, http://www.ensembl.org/index.html (for version 36)
Mouse Genome Informatics, http://www.informatics.jax.org/ (for *Gdf6* [accession number MGI:3604391])
NCBI BLAST, http://www.ncbi.nlm.nih.gov/blast/
NCBI Entrez, http://www.ncbi.nlm.nih.gov/gquery/gquery.fcgi
Online Mendelian Inheritance in Man (OMIM), http://www.ncbi.nlm.nih.gov/Omim/ (for coloboma, CHARGE, *OTX2, SHH, MAF, CHX10, CHD7, PAX6,* Cat eye syndrome, Jacobsen syndrome, Wolf-Hirschhorn syndrome, and *GDF6*)
UCSC Genome Browser, http://genome.ucsc.edu/
UniGene, http://www.ncbi.nlm.nih.gov/entrez/query.fcgi?db=unigene

References

1. Gregory-Evans CY, Williams MJ, Halford S, Gregory-Evans K (2004) Ocular coloboma: a reassessment in the age of molecular neuroscience. J Med Genet 41:881–891
2. Ragge NK, Brown AG, Poloschek CM, Lorenz B, Henderson RA, Clarke MP, Russell-Eggitt I, Fielder A, Gerrelli D, Martinez-Barbera JP, et al (2005) Heterozygous mutations of *OTX2* cause severe ocular malformations. Am J Hum Genet 76:1008–1022
3. Schimmenti LA, de la Cruz J, Lewis RA, Karkera JD, Manligas GS, Roessler E, Muenke M (2003) Novel mutation in sonic hedgehog in non-syndromic colobomatous microphthalmia. Am J Med Genet A 116:215–221
4. Jamieson RV, Perveen R, Kerr B, Carette M, Yardley J, Heon E, Wirth MG, van Heyningen V, Donnai D, Munier F, et al (2002) Domain disruption and mutation of the bZIP transcription factor, MAF, associated with cataract, ocular anterior segment dysgenesis and coloboma. Hum Mol Genet 11:33–42
5. Ferda Percin E, Ploder LA, Yu JJ, Arici K, Horsford DJ, Rutherford A, Bapat B, Cox DW, Duncan AM, Kalnins VI, et al (2000) Human microphthalmia associated with mutations in the retinal homeobox gene CHX10. Nat Genet 25:397–401
6. Vissers LE, van Ravenswaaij CM, Admiraal R, Hurst JA, de Vries BB, Janssen IM, van der Vliet WA, Huys EH, de Jong PJ, Hamel BC, et al (2004) Mutations in a new member of the chromodomain gene family cause CHARGE syndrome. Nat Genet 36:955–957
7. Lalani SR, Safiullah AM, Fernbach SD, Harutyunyan KG, Thaller C, Peterson LE, McPherson JD, Gibbs RA, White LD, Hefner M, et al (2006) Spectrum of *CHD7* mutations in 110 individuals with CHARGE syndrome and genotype-phenotype correlation. Am J Hum Genet 78:303–314
8. Azuma N, Yamaguchi Y, Handa H, Hayakawa M, Kanai A, Yamada M (1999) Missense mutation in the alternative splice region of the PAX6 gene in eye anomalies. Am J Hum Genet 65:656–663
9. Toker E, Elcioglu N, Ozcan E, Yenice O, Ogut M (2003) Colobomatous macrophthalmia with microcornea syndrome: report of a new pedigree. Am J Med Genet A 121:25–30
10. Lehman DM, Sponsel WE, Stratton RF, Mensah J, Macdonald JC, Johnson-Pais TL, Coon H, Reveles XT, Cody JD, Leach RJ (2001) Genetic mapping of a novel X-linked recessive colobomatous microphthalmia. Am J Med Genet 101:114–119
11. Porges Y, Gershoni-Baruch R, Leibu R, Goldscher D, Zonis S, Shapira I, Miller B (1992) Hereditary microphthalmia with colobomatous cyst. Am J Ophthalmol 114:30–34
12. Morlé L, Bozon M, Zech J-C, Alloisio N, Raas-Rothschild A, Philippe C, Lambert J-C, Godet J, Plauchu H, Edery P (2000) A locus for autosomal dominant colobomatous microphthalmia maps to chromosome 15q12-q15. Am J Hum Genet 67: 1592–1597
13. Barros-Nunez P, Medina C, Mendoza R, Sanchez-Corona J, Garcia-Cruz D (1995) Unexpected familial recurrence of iris coloboma: a delayed mutation mechanism? Clin Genet 48: 160–161
14. Eccles MR, Schimmenti LA (1999) Renal-coloboma syndrome: a multi-system developmental disorder caused by PAX2 mutations. Clin Genet 56:1–9
15. Nixon J, Oldridge M, Wilkie AO, Smith K (1997) Interstitial deletion of 2q associated with craniosynostosis, ocular coloboma, and limb abnormalities: cytogenetic and molecular investigation. Am J Med Genet 70:324–327
16. Zollino M, Lecce R, Fischetto R, Murdolo M, Faravelli F, Selicorni A, Buttè C, Memo L, Capovilla G, Neri G (2003) Mapping the Wolf-Hirschhorn syndrome phenotype outside the currently accepted WHS critical region and defining a new critical region, WHSCR-2. Am J Hum Genet 72:590–597
17. Morrison DA, FitzPatrick DR, Fleck BW (2002) Iris coloboma and a microdeletion of chromosome 22: del(22)(q11.22). Br J Ophthalmol 86:1316
18. McTaggart KE, Budarf ML, Driscoll DA, Emanuel BS, Ferreira P, McDermid HE (1998) Cat eye syndrome chromosome breakpoint clustering: identification of two intervals also associated with 22q11 deletion syndrome breakpoints. Cytogenet Cell Genet 81:222–228
19. Pivnick EK, Velagaleti GV, Wilroy RS, Smith ME, Rose SR, Tipton RE, Tharapel AT (1996) Jacobsen syndrome: report of a patient with severe eye anomalies, growth hormone deficiency, and hypothyroidism associated with deletion 11 (q23q25) and review of 52 cases. J Med Genet 33:772–778
20. Fang J, Dagenais SL, Erickson RP, Arlt MF, Glynn MW, Gorski JL, Seaver LH, Glover TW (2000) Mutations in *FOXC2* (*MFH-1*), a forkhead family transcription factor, are responsible for the hereditary lymphedema-distichiasis syndrome. Am J Hum Genet 67:1382–1388
21. Nishimura DY, Swiderski RE, Alward WL, Searby CC, Patil SR, Bennet SR, Kanis AB, Gastier JM, Stone EM, Sheffield VC (1998) The forkhead transcription factor gene *FKHL7* is responsible for glaucoma phenotypes which map to 6p25. Nat Genet 19:140–147

22. Crisponi L, Deiana M, Loi A, Chiappe F, Uda M, Amati P, Bisceglia L, Zelante L, Nagaraja R, Porcu S, et al (2001) The putative forkhead transcription factor *FOXL2* is mutated in blepharophimosis/ptosis/epicanthus inversus syndrome. Nat Genet 27:159–166
23. Fantes J, Ragge NK, Lynch SA, McGill NI, Collin JR, Howard-Peebles PN, Hayward C, Vivian AJ, Williamson K, van Heyningen V, et al (2003) Mutations in *SOX2* cause anophthalmia. Nat Genet 33:461–463
24. Zhou E, Grimes P, Favor J, Koeberlein B, Pretsch W, Neuhauser-Klaus A, Sidjanin D, Stambolian D (1997) Genetic mapping of a mouse ocular malformation locus, Tcm, to chromosome 4. Mamm Genome 8:178–181
25. Wang KS, Zahn LE, Favor J, Huang KM, Stambolian D (2005) Genetic and phenotypic analysis of Tcm, a mutation affecting early eye development. Mamm Genome 16:332–343
26. Speicher MR, Gwyn Ballard S, Ward DC (1996) Karyotyping human chromosomes by combinatorial multi-fluor FISH. Nat Genet 12:368–375
27. Selzer RR, Richmond TA, Pofahl NJ, Green RD, Eis PS, Nair P, Brothman AR, Stallings RL (2005) Analysis of chromosome breakpoints in neuroblastoma at sub-kilobase resolution using fine-tiling oligonucleotide array CGH. Genes Chromosomes Cancer 44:305–319
28. Altschul SF, Gish W, Miller W, Myers EW, Lipman DJ (1990) Basic local alignment search tool. J Mol Biol 215:403–410
29. Schwartz S, Zhang Z, Frazer KA, Smit A, Riemer C, Bouck J, Gibbs R, Hardison R, Miller W (2000) PipMaker—a web server for aligning two genomic DNA sequences. Genome Res 10: 577–586
30. Prince VE, Moens CB, Kimmel CB, Ho RK (1998) Zebrafish hox genes: expression in the hindbrain region of wild-type and mutants of the segmentation gene, valentino. Development 125:393–406
31. Davidson AJ, Postlethwait JH, Yan YL, Beier DR, van Doren C, Foernzler D, Celeste AJ, Crosier KE, Crosier PS (1999) Isolation of zebrafish gdf7 and comparative genetic mapping of genes belonging to the growth/differentiation factor 5, 6, 7 subgroup of the TGF-beta superfamily. Genome Res 9:121–129
32. Rissi M, Wittbrodt J, Delot E, Naegeli M, Rosa FM (1995) Zebrafish radar: a new member of the TGF-beta superfamily defines dorsal regions of the neural plate and the embryonic retina. Mech Dev 49:223–234
33. Hall CJ, Flores MV, Davidson AJ, Crosier KE, Crosier PS (2002) Radar is required for the establishment of vascular integrity in the zebrafish. Dev Biol 251:105–117
34. Sidi S, Goutel C, Peyrieras N, Rosa FM (2003) Maternal induction of ventral fate by zebrafish radar. Proc Natl Acad Sci USA 100:3315–3320
35. Langheinrich U, Hennen E, Stott G, Vacun G (2002) Zebrafish as a model organism for the identification and characterization of drugs and genes affecting p53 signaling. Curr Biol 12: 2023–2028
36. Waskiewicz AJ, Rikhof HA, Moens CB (2002) Eliminating zebrafish pbx proteins reveals a hindbrain ground state. Dev Cell 3:723–733
37. Chang C, Hemmati-Brivanlou A (1999) *Xenopus* GDF6, a new antagonist of noggin and a partner of BMPs. Development 126:3347–3357
38. Stoll C, Alembik Y, Dott B, Roth MP (1997) Congenital eye malformations in 212,479 consecutive births. Ann Genet 40: 122–128
39. Storm EE, Huynh TV, Copeland NG, Jenkins NA, Kingsley DM, Lee SJ (1994) Limb alterations in brachypodism mice due to mutations in a new member of the TGF beta-superfamily. Nature 368:639–643
40. Wolfman NM, Hattersley G, Cox K, Celeste AJ, Nelson R, Yamaji N, Dube JL, DiBlasio-Smith E, Nove J, Song JJ, et al (1997) Ectopic induction of tendon and ligament in rats by growth and differentiation factors 5, 6, and 7, members of the TGF-beta gene family. J Clin Invest 100:321–330
41. Huillard E, Laugier D, Marx M (2005) Defects in chicken neuroretina misexpressing the BMP antagonist Drm/Gremlin. Dev Biol 283:335–344
42. Schedl A, Ross A, Lee M, Engelkamp D, Rashbass P, van Heyningen V, Hastie ND (1996) Influence of PAX6 gene dosage on development: overexpression causes severe eye abnormalities. Cell 86:71–82
43. Smith RS, Zabaleta A, Kume T, Savinova OV, Kidson SH, Martin JE, Nishimura DY, Alward WL, Hogan BL, John SW (2000) Haploinsufficiency of the transcription factors FOXC1 and FOXC2 results in aberrant ocular development. Hum Mol Genet 9:1021–1032
44. Nishimura DY, Searby CC, Alward WL, Walton D, Craig JE, Mackey DA, Kawase K, Kanis AB, Patil SR, Stone EM, et al (2001) A spectrum of *FOXC1* mutations suggests gene dosage as a mechanism for developmental defects of the anterior chamber of the eye. Am J Hum Genet 68:364–372
45. Lehmann OJ, Ebenezer ND, Ekong R, Ocaka L, Mungall AJ, Fraser S, McGill JI, Hitchings RA, Khaw PT, Sowden JC, et al (2002) Ocular developmental abnormalities and glaucoma associated with interstitial 6p25 duplications and deletions. Invest Ophthalmol Vis Sci 43:1843–1849
46. Lehmann OJ, Ebenezer ND, Jordan T, Fox M, Ocaka L, Payne A, Leroy BP, Clark BJ, Hitchings RA, Povey S, et al (2000) Chromosomal duplication involving the forkhead transcription factor gene *FOXC1* causes iris hypoplasia and glaucoma. Am J Hum Genet 67:1129–1135
47. Settle SH Jr, Rountree RB, Sinha A, Thacker A, Higgins K, Kingsley DM (2003) Multiple joint and skeletal patterning defects caused by single and double mutations in the mouse Gdf6 and Gdf5 genes. Dev Biol 254:116–130
48. Brown DJ, Kim TB, Petty EM, Downs CA, Martin DM, Strouse PJ, Moroi SE, Milunsky JM, Lesperance MM (2002) Autosomal dominant stapes ankylosis with broad thumbs and toes, hyperopia, and skeletal anomalies is caused by heterozygous nonsense and frameshift mutations in *NOG,* the gene encoding noggin. Am J Hum Genet 71:618–624
49. Woodward KJ, Cundall M, Sperle K, Sistermans EA, Ross M, Howell G, Gribble SM, Burford DC, Carter NP, Hobson DL, et al (2005) Heterogeneous duplications in patients with Pelizaeus-Merzbacher disease suggest a mechanism of coupled homologous and nonhomologous recombination. Am J Hum Genet 77:966–987
50. Lee JA, Inoue K, Cheung SW, Shaw CA, Stankiewicz P, Lupski JR (2006) Role of genomic architecture in PLP1 duplication causing Pelizaeus-Merzbacher disease. Hum Mol Genet 15: 2250–2265
51. Wadman M (2006) Medical research: them and us no longer. Nature 439:779–780
52. Varki A, Holmes E, Yamada T, Agre P, Brenner S (2006) Physician-scientists are needed now more than ever. Nature 440: 740
53. Hanel ML, Hensey C (2006) Eye and neural defects associated with loss of GDF6. BMC Dev Biol 6:43